ORAL/POSTER REFERENCE: 001053OR

Crack initiation behavior of piezoelectric ceramics: electro-mechanical interaction

B. Liu[1], Z.F. Song[2], G.C. Sih[1,2,3]

[1] Institute of Engineering Mechanics, Hebei University of Technology, Tianjin, 300130, China
[2]School of Advanced Science and Technology, Xi’an Jiaotong University, Xi’an, 710049, China
[3]Institute of Mechanics, Chinese Academy of Sciences, Beijing 100080, China

ABSTRACT

Crack initiation behavior in piezoelectric ceramics is examined for different choices of boundary conditions. They are referred to as the fundamental boundary-value problems when electric field/stress and electric displacement/strain are specified. The mixed boundary-value problems involve specifying electric displacement/stress and electric field/strain. Crack-growth is assumed to occur when the volume energy density function that accounts for interaction of mechanical and electrical effects reaches a threshold depending on the piezoelectric ceramic material properties. The crack driving force is shown to increase monotonically for positive and negative applied electric displacement or electric field. Such a trend prevails for the fundamental boundary-value problems as it is to be expected on physical grounds. The applied electric field and displacement have little influence on the energy density solution for the mixed boundary conditions.

KEYWORDS

Anti-plane shear, Crack growth, Electric-mechanical coupling, Piezoelectric ceramics, Shear stress

1. INTRODUCTION

Piezoelectric ceramics can be made to have “pole” directions where the dipole moments are aligned. These directions need not coincide with those of material anisotropy. Their interactions could involve a rotation and/or reflection of axes depending on whether the deformation is of the in-plane or out-of-plane type. A special feature of electrical and mechanical interplay is that a piezoelectric material could produce an electric field when deformed and vice versa. This makes piezoelectric ceramics attractive for making electronic devices that may include transducers, sensors, etc. Their reliability in service, however, can often be short changed by premature cracking. To this end, much attention has been given to analyzing the state of affairs near a sharp crack and the condition under which an existing crack would start to propagate. Past works [1-5] have reported inconsistencies between analytical and experimental results, particularly those concerned with application of the classical energy release rate concept. More recent works [6-10] showed that the energy density criterion had more success for resolving several of the previously unexplained fracture phenomena.

Solutions based on linear piezoelasticity theory have shown that the stress, strain, electric displacement and electric fields possess the inverse square root of r singularity at a sharp crack tip. Here, r stands for the radial distance measured from the crack front. The ways with which the aforementioned four boundary conditions affect crack initiation have been discussed and analyzed using different approaches. Widely applied in the literature [1-5] is the energy release rate criterion. It relies on the exchange of global energy with the increase of local crack surface area. When electro-mechanical coupling effects are present, it is not apparent whether all the energy would be converted to the creation of new crack surface. This is similar to elasto-plastic fracture where the plastic energy being part of the total energy does not contribute to the increase of crack surface. It is involved only in a passive manner to reduce a portion of the total energy that would have otherwise be present in crack surface extension. Such a distinction is not and cannot be made in the energy release rate treatment. Linear theory has often been blamed as the scape goat for inadequacies that are embedded in the failure/fracture criterion, not because of the lack of nonlinearity.

The volume energy density criterion [11,12] does not have the inherent constraint of applying a global energy quantity to determine local crack driving force unless all of the energy is converted to the increase of crack surface. It focuses attention on the failure of a local element. Crack extension is regarded as the loci of failed elements. The global energy is not involved locally although the correct stress-strain analysis has to be made for determining the local stress and strain fields.

2. TRACTION AND CHARGE FREE CRACK

The anti-plane shear crack model has been used extensively in fracture mechanics because of its simplicity in formulation. Referring to Fig. 1(a), a line crack of length 2a is centered in a large body that is assumed to extend to infinity in all direction x, y, and z.

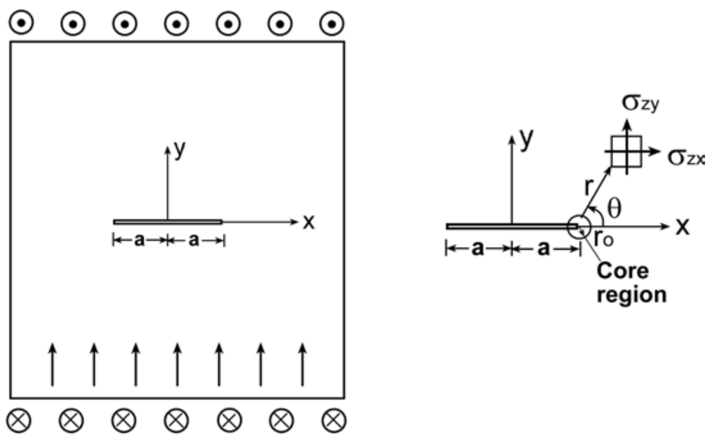

(a) Applied electric and mechaical load (b) Local coordinates

Fig. 1 Mode III crack line

2.1 Boundary conditions

The body is sheared at infinity with mechanical stress τ_∞ or strain γ_∞. Either electric displacement D_∞ or electric field E_∞ is applied in conjunction with the mechanical stress τ_∞ or strain γ_∞. The four possible combinations are ($\tau_\infty;E_\infty$), ($\gamma_\infty;D_\infty$), ($\tau_\infty;D_\infty$) and ($\gamma_\infty;E_\infty$). They will be referred to, respectively, as Case I, II, III and IV. This is summarized in Table 1. The corresponding quantities F_j and G_j (j = I, II, etc.) are given by

$$F_I = \frac{\tau_\infty + e_{15}E_\infty}{c_{44}}, \quad F_{II} = \gamma_\infty, \quad F_{III} = \frac{\in_{11}\tau_\infty + e_{15}D_\infty}{c_{44}\in_{11} + e_{15}^2}, \quad F_{IV} = \gamma_\infty \tag{1}$$

and

$$G_I = E_\infty, \quad G_{II} = \frac{D_\infty - e_{15}\gamma_\infty}{\in_{11}}, \quad G_{III} = \frac{c_{44}D_\infty - e_{15}\tau_\infty}{c_{44}\in_{11} + e_{15}^2}, \quad G_{IV} = E_\infty \tag{2}$$

TABLE 3
Classification of boundary conditions

Cases	Specified quantities	Intensity factor coeff.
Fundamental problems		
I	τ_∞ and E_∞	F_I ; G_I
II	γ_∞ and D_∞	F_{II} ; G_{II}
Mixed problems		
III	τ_∞ and D_∞	F_{III} ; G_{III}
IV	γ_∞ and E_∞	F_{IV} ; G_{IV}

Eqs. (1) and (2) are coefficients that define the stress, strain, electric field and displacement factors in the work to follow.

More specifically, the boundary conditions are

$$\sigma_{zy} = \tau_\infty \ \text{or} \ \gamma_{zy} = \gamma_\infty \ \text{for} \ x^2 + y^2 \to \infty \tag{3}$$

together with

$$E_y = E_\infty \ \text{or} \ D_y = D_\infty \ \text{for} \ x^2 + y^2 \to \infty \tag{4}$$

For a crack free of surface tractions and charge (i.e., an insulated crack), the conditions are

$$\sigma_{zy} = 0, \ D_y = 0 \ \text{for} \ |x| < a; \quad |y| = 0 \tag{5}$$

The pole is directed along the z-axis as shown in Fig. 1(b). Reversing the direction of E_∞ and D_∞ is equivalent to reversing the direction of poling.

2.2 Asymptotic solution

It can be solved for the two unknowns u_z and ϕ from which the stresses, strains, electric field and displacements throughout the medium can be obtained. For the present discussion, it suffices to consider the asymptotic expressions [5]:

$$\sigma_{zx} = -\frac{K_{III}^{\tau}}{\sqrt{2\pi r}}\sin(\frac{\theta}{2}), \quad \sigma_{zy} = \frac{K_{III}^{\tau}}{\sqrt{2\pi r}}\cos(\frac{\theta}{2}) \tag{6}$$

$$\gamma_{zx} = -\frac{K_{III}^{\gamma}}{\sqrt{2\pi r}}\sin(\frac{\theta}{2}), \quad \gamma_{zy} = \frac{K_{III}^{\gamma}}{\sqrt{2\pi r}}\cos(\frac{\theta}{2}) \tag{7}$$

and

$$E_x = -\frac{K_E}{\sqrt{2\pi r}}\sin(\frac{\theta}{2}), \quad E_y = \frac{K_E}{\sqrt{2\pi r}}\cos(\frac{\theta}{2}) \tag{8}$$

$$D_x = -\frac{K_D}{\sqrt{2\pi r}}\sin(\frac{\theta}{2}), \quad D_y = \frac{K_D}{\sqrt{2\pi r}}\cos(\frac{\theta}{2}) \tag{9}$$

The stress and strain intensity factors in eqs. (6) and (7) are defined by

$$K_{III}^{\tau} = (c_{44}F_j - e_{15}G_j)\sqrt{\pi a}, \quad K_{III}^{\gamma} = F_j\sqrt{\pi a} \tag{10}$$

where j = I, II, etc. The electric field and displacement factors in eqs. (8) and (9) are given by

$$K_E = G_j\sqrt{\pi a}, \quad K_D = (e_{15}F_j + \epsilon_{11}\, G_j)\sqrt{\pi a} \tag{11}$$

The electro-mechanical coupling effects are included by the factors in eqs. (10) and (11) via the constants F_j

and G_j given in eqs. (1) and (2). The local polar coordinates (r,θ) in eqs. (6) to (9) are measured from the crack tips; they are shown in Fig. 1(a). Note that all quantities possess the $1/\sqrt{r}$ singularity, a characteristic that is unaffected by piezoelectricity. In this case, the angular functions of the stresses and strains in eqs. (6) and (7) are also the same as those for purely elastic materials.

4. VOLUME ENERGY DENSITY APPROACH

According to the volume energy density criterion [9,10], attention is focused on the failure of an element nearest to the crack tip as shown in Fig. 1(a). Linear piezoelasticity provides the expression:

$$\frac{dW}{dV} = \frac{1}{2}\sigma_{ij}\gamma_{ij} + \frac{1}{2}D_i E_i \tag{12}$$

which simplifies considerably for anti-plane shear deformation:

$$\frac{dW}{dV} = \frac{1}{2}(\sigma_{xz}\gamma_{xz} + \sigma_{yz}\gamma_{yz}) + \frac{1}{2}(D_x E_x + D_y E_y) \tag{13}$$

Since the right hand side of eq. (13) are known from eqs. (6) to (9) inclusive, dW/dV can be computed with the aid of eqs. (1) and (2).

4.1 Crack initiation threshold

In view of the singular behavior of the quantities in eqs. (6) to (9), dW/dV is proportional to 1/r which tends to be become unbounded as $r \to 0$. Unboundness of dW/dV is excluded from the solution by letting $r \to r_o$ being the limit of r. For small values of r, the volume energy density can thus be written as

$$\frac{dW}{dV} = \frac{S}{r} \tag{14}$$

in which S is known as the energy density factor. It may be regarded as the crack driving force. For $r = r_o$, it suffices to examine S for the condition of crack initiation. if only mechanical shear stress τ_∞ is applied, then dW/dV can be computed simply as

$$\frac{dW}{dV} = \left(\frac{a\tau_\infty^2}{4c_{44}}\right)\frac{1}{r} \tag{15}$$

which gives $S = a\tau_\infty^2/(4c_{44})$. The onset of crack initiation would be assumed to coincide with $S = S_c$, a critical value while τ_∞ would correspond to the critical shear stress. for an isotropic elastic material c_{44} corresponds to the shear modulus of elasticity and $S = a\tau_\infty^2/(4G)$ [13].

4.2 Boundary-value problems

Let p_τ and q_γ stand for the ratios E_∞/τ_∞ and D_∞/γ_∞, respectively. By means of eqs. (13) and (14), S can be calculated from the asymptotic expressions in eqs. (6) to (9). the results for Case I and II in Table 1 take the forms

$$S = \frac{a}{4}\begin{cases} \dfrac{\tau_\infty^2}{c_{44}}[1 + 2e_{15}p_\tau + (c_{44}\in_{11} + e_{15}^2)p_\tau^2], & \text{Case I} \qquad (16) \\ \dfrac{\gamma_\infty^2}{\in_{11}}[(c_{44}\in_{11} + e_{15}^2) - 2e_{15}q_\gamma + q_\gamma^2], & \text{Case II} \qquad (17) \end{cases}$$

Similarly, let p_γ and q_τ stand for the ratio E_∞/γ_∞ and D_∞/τ_∞, respectively. In the same way, the S-factor expressions for Case III and IV are

$$
S=\frac{a}{4}\begin{cases}\gamma_\infty^2[c_{44}+\in_{11}p_\gamma^2], & \text{Case III} \quad (18)\\ \dfrac{\tau_\infty^2}{c_{44}\in_{11}+e_{15}^2}[\in_{11}+c_{44}q_\tau^2], & \text{Case IV} \quad (19)\end{cases}
$$

The condition of a uniform electric field can be more readily simulated at the surface of the piezoelectric material in contrast to the electric displacement boundary condition. Frequently used in the laboratory is Case I in eq. (16).

4.3 PZT-5H piezoceramic

A glance of eqs. (16) to (19) reveals that only three constants c_{44}, e_{15} and $\in_{11}$ are involved for the anti-shear problem. Their numerical values for the lead zirconate titante (PZT-5H) piezoceramic can be found in Table 2 [14].

TABLE 2
Constants of PZT-5H piezoceramic [14]

c_{44} (N/m^2)	e_{15} (C/m^2)	$\in_{11}$ (C/Vm^2)
3.53×10^{10}	17.0	151×10^{-10}

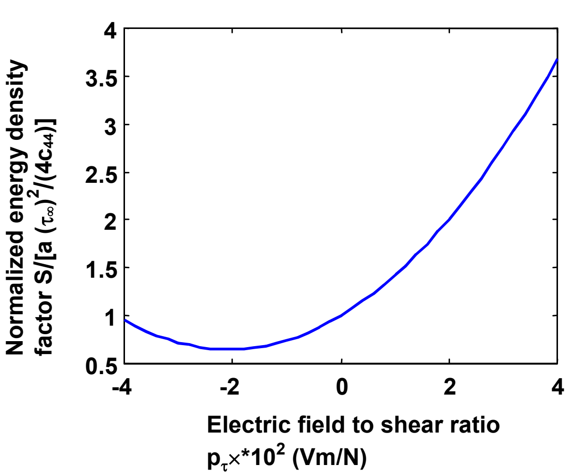

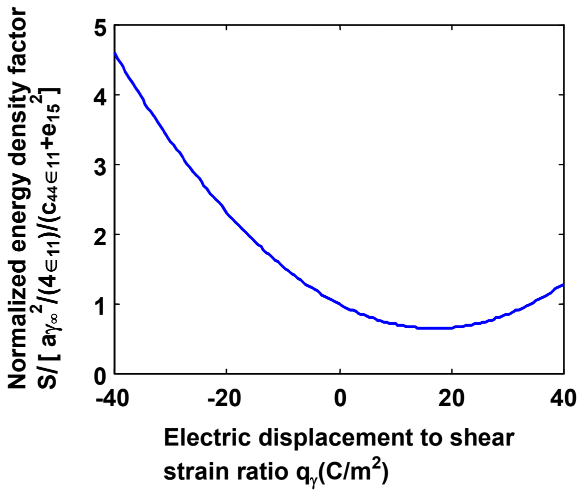

Figure 2: Normalized energy density factor versus E_∞/τ_∞ **Figure 3:** Normalized energy density factor versus D_∞/γ_∞

Plotted in Fig. 2 are the variations of the normalized volume energy density factor $S_c/(a\tau_\infty^2/4c_{44})$ with the load parameter E_∞/τ_∞. In general, the curve rises as p_τ is increased positively or negatively; it possesses a minimum for negative p_τ very close to the origin. On physical grounds, the crack driving force represented by S would increase with increasing applied electric field. Similar results are obtained for $S_c/(a\gamma_\infty^2/4\in_{44})$ versus D_∞/γ_∞ as shown in Fig. 3 where the minimum corresponds to positive q_τ near the origin. As it is to be expected, S increases for positive and negative applied electric displacements. The trends of the curves in Figs. 2 and 3 are opposite to those found in [5] by using the energy release rate criterion where the crack driving forces decrease and become negative when the applied electric field and displacement are increased. This is contrary to experimental observations.

Refering to the material parameters in Table 2, it can be seen that $\in_{11}$ is several orders of magnitude smaller than c_{44} in eq. (27) for Case III. Hence, S would remain nearly constant and not affected by the ratio E_∞/γ_∞. Case IV in eq. (19) yields a symmetric curve about $q_\tau = 0$ for the S versus q_τ plot. The mixed conditions in eqs. (18) and (19) are only of academic interest since they are difficult to produce in the laboratory.

5. CONCLUSIONS

Anti-plane shear crack initiation behavior for piezoceramics is investigated to study the electro-mechanical interaction effects. Applied is the volume energy density criterion for analyzing how different boundary conditions would affect the crack driving force which remains positive definite under all conditions. This is a necessary requirement that must be satisfied on physical grounds. Numerical results are presented graphically for the PZT-5H piezoelectric material. These conclusions are contrary to those obtained from the energy release rate criterion [5] for the same problem. The crack energy release rate becomes negative as the electric field or displacement is increased, a condition that seems to contradict rational reasoning. In other words, it is inconceivable that a crack would arrest if the applied electric and/or mechanical load is increased. These unphysical predictions invalidate the usefulness of the energy release rate. Such contradictions do not arise when the volume energy density criterion is used.

REFERENCES

[1] Z. Suo, C. M. Kuo, D. M. Barnett and J. R. Willis, Fracture mechanics for piezoelectric ceramics. J. Mech. Phys. Solids, 40 (1992), 739-765.
[2] Y. E. Pak and A. Tobin, On the electric field effects in fracture of piezoelectric materials. Mechanics of Electromagnetic Materials and Structures, AMD-Vol.161/MD-Vol.42, ASME, 1993.
[3] H. Gao, T. Y. Zhang and P. Tong, Local and global energy release rates for an electrically yielded crack in a piezoelectric ceramic. J. Mech. Phys. Solids, 45 (1997), 491-510.
[4] S. Park and C. T. Sun, Fracture criterion of piezoelectric ceramics. J. Am. Ceram. Soc., 78 (1995), 1475-1480.
[5] Y.E. Pak, Crack extension force in a piezoelectric material, J. of Applied Mechanics, 57(1990) 647-653.
[6] S. Shen and T. Nishioka, Fracture of piezoelectric materials: energy density criterion, J. Theoretical Appl. Fract. Mech., Vol.33(1) (2000), 57-63.
[7] Z.T. Chen, Anti-plane mechanical and in-plane electric time –dependent load applied to two coplanar cracks in piezoelectric ceramic material, J. of Theoretical and Applied Fracture Mechanics, 33 (3) (2000), 173-184.
[8] B.L. Wang, N. Noda, Crack initiation in PZT-4 piezoelectric ceramic strip, J. of Theoretical and Applied Fracture Mechanics, 33 (1) (2000), 35-47.
[9] J.Z. Zuo and G.C. Sih, Energy density formulation and interpretation of cracking behavior for piezoelectric ceramics, J. of Theoretical and Applied Fracture Mechanics, 34 (1) 2000, 17-33.
[10] G.C. Sih, J.Z Zuo, Multiscale behavior of crack initiation and growth in piezoelectric ceramics, J. of Theoretical and Applied Fracture Mechanics, 34(2000) 123-141.
[11] G.C. Sih, Mechanics of Fracture, Volume I to VII, Sijhoff and Noordhoff International Publisher, The Netherlands, 1973-1981.
[12] G.C. Sih, Mechanics of fracture initiation and propagation, Kluwer Academic Publishers, The Netherlands, 1991.
[13] G.C. Sih, Fracture mechanics of engineering structural components, Fracture Mechanics Methodology, G.C. Sih, L. Faria, eds., Martinus Nijhoff Publishers, The Netherlands, 35-101 (1984).
[14] R.C. Pohanka, P.L. Smith, Recent advances in piezoelectric ceramics, Electronic Ceramics, L.M. Levinson, ed., Marcel Dekker, New York, 1988.